

Amphiphilic Cylindrical Core–Shell Brushes via a “Grafting From” Process Using ATRP

Guanglou Cheng,[†] Alexander Böker,^{†,‡} Mingfu Zhang,[†] Georg Krausch,^{‡,§} and Axel H. E. Müller^{*,†,§}

Makromolekulare Chemie II, Physikalische Chemie II, and Bayreuther Zentrum für Kolloide und Grenzflächen, Universität Bayreuth, D-95440 Bayreuth, Germany

Received August 8, 2000; Revised Manuscript Received July 10, 2001

ABSTRACT: Atom transfer radical polymerization (ATRP) was applied to the synthesis of amphiphilic cylindrical polymer brushes by using the “grafting from” technique. The procedure included the following steps: (1) ATRP of 2-hydroxyethyl methacrylate (HEMA) gave well-defined poly(HEMA), (2) subsequent esterification of the pendant hydroxy groups of poly(HEMA) with 2-bromoisobutyryl bromide yielded a polyinitiator, poly(2-(2-bromoisobutyryloxy)ethyl methacrylate) (PBIEM), (3) ATRP of various monomers (*tert*-butyl acrylate, or styrene) using PBIEM as polyinitiator yielded cylindrical brushes with homopolymer side chains, (4) addition of a second monomer (styrene or *tert*-butyl acrylate) formed the cylindrical brushes with diblock copolymer side chains (core–shell cylinders), and (5) hydrolysis of the poly(*tert*-butyl acrylate) (P*t*BA) block of the side chains to poly(acrylic acid) (PAA) formed amphiphilic core–shell polymer brushes. By using this technique, well-defined core–shell cylindrical polymer brushes with polystyrene (PS), P*t*BA, PS-*b*-P*t*BA, P*t*BA-*b*-PS, PS-*b*-PAA, or PAA-*b*-PS as side chains were successfully synthesized. The molecular weights and radii of gyration of the polymer brushes were obtained by static light scattering in THF. The absence of inter/intra-macromolecular coupling reactions during ATRP synthesis was confirmed by GPC, NMR, and MALDI–TOF analyses of the side chains and scanning force microscopy (SFM). Single wormlike unimolecular nanocylinders are clearly visualized on a mica surface while aggregates are usually observed on a SiO_x surface. The brushes with PS-*b*-P*t*BA side chains were hydrolyzed to PS-*b*-PAA side chains forming unimolecular wormlike micelles. These unimolecular micelles showed a unique response to solvent quality, as indicated by ¹H NMR and dynamic light scattering.

Introduction

Cylindrical polymer brushes have received considerable attention.^{1–8} Typically, these brushes were synthesized via conventional free-radical polymerization of macromonomers, which were obtained by ionic, group transfer, or ring-opening metathesis polymerization. Amphipolar cylindrical core–shell brushes were also obtained by free-radical polymerization of amphiphilic diblock macromonomers.⁹ However, this method is ill-controlled in the degree of polymerization (DP) of the produced polymacromonomer, so the crude product may contain polymers with both starlike and brushlike shapes in addition to residual macromonomers.¹⁰ SEC fractionation is needed to obtain brushes with narrow molecular weight distribution (MWD),⁸ which then can be cast onto a surface to form highly ordered films.

Recently, Beers et al.¹¹ reported the synthesis of well-defined polymer brushes with poly(*n*-butyl acrylate) or polystyrene side chains via ATRP grafting from a polyinitiator, poly(2-(2-bromoisobutyryloxy)ethyl methacrylate) (PBIEM), which was obtained by the esterification of poly[2-(trimethylsilyloxy)ethyl methacrylate] (PTMSHEMA). This method allows the control of the length and the composition of both the backbone and the side chains.

Here we report the synthesis and characterization of well-defined cylindrical core–shell polymer brushes via ATRP.²² The resulting brushes with diblock copolymer

side chains can be easily hydrolyzed to amphiphilic core–shell nanocylinders, which may find use for a number of applications in nanotechnology, e.g., use as cylindrical nanoreactors with well-defined dimensions for the synthesis of novel nanosized organic/inorganic hybrid systems.

Experimental Part

Materials. 2-Hydroxyethyl methacrylate (HEMA, Acros, 96%) was purified according to the literature.^{12a} *tert*-Butyl acrylate (*t*BA, BASF AG) was fractionated from CaH₂ at 45 mbar, stirred over CaH₂, degassed, and distilled in a high vacuum. Styrene (Acros, 99%) was vacuum distilled just before use. CuBr (95%, Aldrich) was purified by stirring overnight in acetic acid. After filtration, it was washed with ethanol and diethyl ether and then dried. α -Bromoisobutyryl bromide, 2,2'-bipyridine (bpy), 1,1,4,7,10,10-hexamethyltriethylenetetramine (HMTETA), and *N,N,N',N'*-pentamethyldiethylenetriamine (PMDETA) were purchased from Aldrich and used as received without further purification. Poly(2-hydroxyethyl methacrylate) (poly(HEMA)) was prepared in ethanol by ATRP using CuBr/HMTETA catalyst, according to the literature.^{12a} ¹H NMR (CD₃OD): δ = 3.98 (–CH₂–OCO), 3.81 (–CH₂–OH), 2.20–1.40 (–CH₂–C), 1.30–0.70 (–CH₃) ppm.

Preparation of Poly(2-(2-bromoisobutyryloxy)ethyl methacrylate) (PBIEM).¹³ A 8.1 g sample of poly(HEMA) (–OH groups, 0.0623 mol) was dissolved in 100 mL of anhydrous pyridine. Then 28.6 g (0.124 mol) of α -bromoisobutyryl bromide was added dropwise at 0 °C in 60 min. The mixture was stirred for 3 h at 0 °C followed by stirring at room temperature for 24 h. The insoluble salt was then removed by filtration, and the solvent was removed by a rotating evaporator. The produced polymer was purified by passing through an Al₂O₃ column using toluene as solvent, followed by precipitation in methanol. Yield: 81.3%. GPC (against PS standards): M_n = 29 150; M_w/M_n = 1.24. Membrane osmometry:

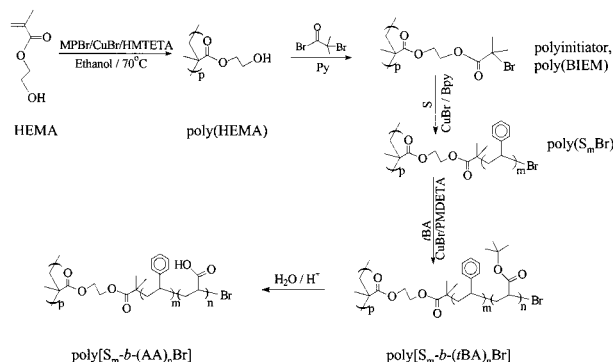
* Corresponding author. E-mail: axel.mueller@uni-bayreuth.de.

[†] Makromolekulare Chemie II, Universität Bayreuth.

[‡] Physikalische Chemie II, Universität Bayreuth.

[§] Bayreuther Zentrum für Kolloide und Grenzflächen, Universität Bayreuth.

Scheme 1



$M_n = 86\,760$. $^1\text{H NMR}$ (CDCl_3): $\delta = 4.31, 4.14$ ($-\text{CH}_2-\text{OCO}$), $2.20-1.40$ ($-\text{CH}_2-\text{C}$), 1.97 [$-\text{C}(\text{Br})(\text{CH}_3)_2$], $1.30-0.70$ ($-\text{CH}_3$) ppm.

Typical ATRP Procedure.^{14,15} All operations were carried out under nitrogen atmosphere. CuBr, PMDETA or bipyridine, monomer, initiator, and octane (internal standard, 1/10 molar ratio relative to monomer) were added into a round flask which was then sealed and immersed in an oil bath at a desired temperature for a certain time. After polymerization, the catalyst was removed by an adsorption filtration through a neutral alumina column and the resulting polymer was precipitated in methanol. The solvent was removed by filtration, and the produced polymer was dissolved in benzene and finally freeze-dried.

Hydrolysis of the Brush with PS Side Chains.¹⁶ A 0.32 g sample of the brush with PS side chains ($M_{w,\text{SLS}} = 1.20 \times 10^6$) was dissolved in 40 mL of THF in a 250 mL round flask fitted with a condenser and N_2 inlet. Then 10 mL of KOH solution (1 M in ethanol) was added and the charge refluxed for 72 h. After evaporation to dryness, the polymer was dissolved in THF and then precipitated into acidified methanol and dried under vacuum. GPC (against PS standards): $M_n = 3320$, $M_w/M_n = 1.16$. $^1\text{H NMR}$ (CDCl_3): $\delta = 7.10-6.40$ ($-\text{C}_6\text{H}_5$), $6.17-6.04$ ($-\text{CH}=\text{CH}-\text{C}_6\text{H}_5$), 1.87 [$-\text{CH}(\text{C}_6\text{H}_5)-$], 1.43 [$-\text{CH}_2-\text{CH}(\text{C}_6\text{H}_5)-$], $0.95, 0.85$ [$-\text{C}(\text{CH}_3)_2-$] ppm. MALDI-TOF: $m/z = 87.10$ ($-\text{C}(\text{CH}_3)_2\text{COOH}$) + $n \times 104.15$ (PS backbone) + 103.15 ($-\text{CH}=\text{CH}-\text{C}_6\text{H}_5$) + 107.87 (Ag^+).

Analysis. Monomer conversion was determined by gas chromatography (GC) from the concentration of residual monomer, with octane as an internal standard, using a polymethylsiloxane capillary column. Membrane osmometry was performed in toluene using a cellulose triacetate membrane. Gel permeation chromatography (GPC) was performed using THF as eluent at a flow rate of 1.0 mL/min at room temperature. Column set: 5 μm PSS SDV gel, 10^5 , 10^4 , 10^3 , 10^2 Å, 30 cm each. Detectors: Waters 410 differential refractometer and Waters photodiode array detector operated at 254 nm. PS standards (PSS, Mainz, Germany) were used for the calibration of the column set. Matrix-assisted laser desorption/ionization time-of-flight mass spectrometry (MALDI-TOF MS)

was carried out on a Bruker reflex III spectrometer incorporating a 337 nm nitrogen laser with a 3 ns pulse duration (10^6-10^7 W/cm², 100 μm spot diameter). The instrument was operated in a linear mode with an accelerating potential of 33.65 kV.¹⁷ Dihydroxybenzoic acid was used as a matrix and silver trifluoroacetate as a cationization agent. Proton nuclear magnetic resonance ($^1\text{H NMR}$) spectra were recorded with a Bruker AC-250 spectrometer at room temperature in CDCl_3 . The samples for scanning force microscopy (SFM) measurements were prepared by dip-coating from a dilute solution of polymer in different solvents, with a weight concentration of $10^{-6}-10^{-5}$ g/g, onto a snow-jetted SiO_x surface or a freshly cleaved mica surface. The SFM images were taken with a Digital Instruments Dimension 3100 microscope operated in tapping mode (free amplitude of the cantilever ≈ 30 nm, set point ratio ≈ 0.98). Static light scattering (SLS) experiments were carried out on a Sofica goniometer using a He-Ne laser ($\lambda_0 = 632.8$ nm). The refractive index increment, dn/dc , was measured with the NFT ScanRef interferometer (except for the sample $\text{P}(\text{S}_{23}\text{Br})$, which was measured with a Chromatix KMX-16 laser differential refractometer). Dynamic light scattering (DLS) was performed on an ALV DLS/SLS-SP 5022F compact goniometer system using an ALV 5000/E correlator and a He-Ne laser ($\lambda_0 = 632.8$ nm). Prior to the light scattering measurements the sample solutions were filtered using Millipore Teflon filters with a pore size of 0.45 μm .

Results and Discussion

Synthesis. The synthetic route for brushes with PS core and P(tBA) (or PAA) shell is outlined in Scheme 1. By simply reversing the polymerization sequence of the two monomers, we also synthesized the brush with P(tBA) (or PAA) core and PS shell. We chose 2-hydroxyethyl methacrylate (HEMA) instead of TMSHEMA to form the precursor for polyinitiator (PBIEM) because it can also be easily polymerized by ATRP in ethanol.¹² The final product PBIEM has an apparent number-average molecular weight $M_n = 29\,150$ and polydispersity index $M_w/M_n = 1.24$ against linear PS standards, while the true M_n from osmometry is 86 760. Thus, the backbone of PBIEM has a number-average degree of polymerization $\text{DP}_n = 310$.

Table 1 presents the results of ATRP by using PBIEM as polyinitiator or $\text{P}(\text{S}_m\text{Br})$ and $\text{P}[(\text{tBA})_n\text{Br}]$ as poly-(macroinitiator)s. The obtained polymer brushes with homopolymer or diblock copolymer side chains show monomodal GPC eluograms (Figure 1) and their molecular weight distributions are low ($\text{PDI} < 1.5$), indicating that intermacromolecular coupling reactions are negligible. It seems that, without adding Cu(II) salts,¹¹ a high ratio of monomer to initiator and a low conversion are sufficient to suppress undesirable side reactions, and therefore to obtain the desired brushes with homopolymer or diblock copolymer side chains. To get the true

Table 1. Conditions and Results of ATRP from PBIEM Polyinitiator with $\text{DP}_n = 310$ and $\text{PDI} = 1.24$ and Various Poly(macroinitiator)s

polyinitiator or poly(macroinitiator)	monomer	[CuBr]:[PMDETA]:[Br] ^a : [M]	T (°C)	time (min)	convn (%)	$M_{n,\text{calc}}^b \times 10^5$	$M_{n,\text{NMR}}^c \times 10^5$	$M_{n,\text{GPC}}^d \times 10^5$	PDI ^d	$M_{w,\text{SLS}}^e \times 10^5$	formula ^f
PBIEM	tBA	0.5:0.5:1:300	50	25	12.5	15.6	12.8	2.73	1.47	33.4	$\text{P}[(\text{tBA})_{55}\text{Br}]$
		0.5:0.5:1:300	50	13	6.0	7.96	8.82	2.60	1.36	32.4	$\text{P}[(\text{tBA})_{58}\text{Br}]$
		0.3:0.3:1:200	30	13	3.9	3.98	4.09	1.45	1.42	11.9	$\text{P}[(\text{tBA})_{19}\text{Br}]$
$\text{P}[(\text{tBA})_{19}\text{Br}]$	S	0.5:1.5(bpy):1:300	95	70	4.1	4.86	4.75	1.44	1.45	12.0	$\text{P}(\text{S}_{23}\text{Br})$
		1.0:4.0:1:600	80	70	5.0	12.9	15.1	4.39	1.44		$\text{P}[(\text{tBA})_{19}\text{-b-S}_{81}\text{Br}]^g$
$\text{P}(\text{S}_{23}\text{Br})$	tBA	1.0:4.0:1:500	70	60	10.1	24.6	43.7	4.31	1.34		$\text{P}[\text{S}_{23}\text{-b-(tBA)}_{186}\text{Br}]^g$
		1.0:4.0:1:500	50	25	4.0	12.7	19.5	3.62	1.39	36.8	$\text{P}[\text{S}_{23}\text{-b-(tBA)}_{46}\text{Br}]$

^a Molar concentration of initiating bromine groups. ^b Obtained from GC conversion by assuming the brushes to be formed at all initiating sites. ^c From $^1\text{H NMR}$ in Figure 3. ^d Calibrated against linear PS standards. ^e Measured by static light scattering in THF. ^f Calculation method: example $\text{P}[(\text{tBA})_{55}\text{Br}]$, $M_n = M_{w,\text{SLS}}/\text{PDI}$, $\text{DP}_{\text{side chain}} = (M_n/310 - 279)/128 = 55$, where 279 is the molar mass of the unit of polyinitiator, and 128 is the molar mass of tBA. ^g Obtained from the formula of poly(macroinitiator) and the ratio of two blocks from $^1\text{H NMR}$.

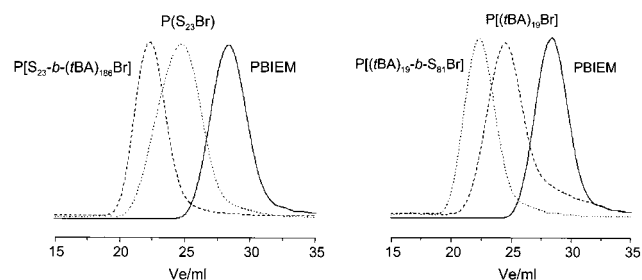


Figure 1. GPC traces of polyinitiator (PBIEM) and of polymer brushes in THF.

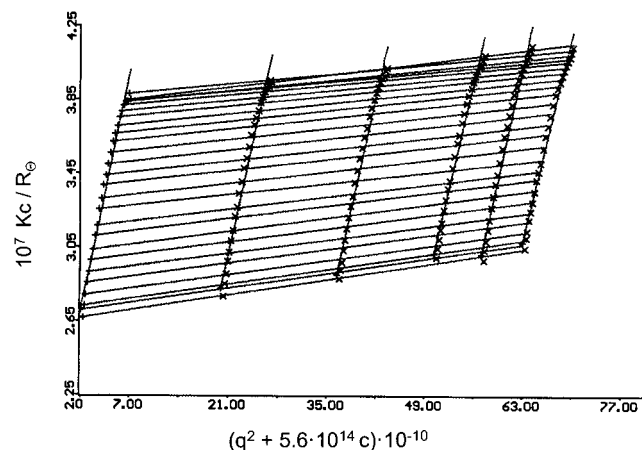


Figure 2. Zimm plot of P[S₂₃-*b*-(tBA)₄₆Br] in THF. $M_w = 3.68 \times 10^6$, $R_g = 45$ nm, and $A_2 = 1.59 \times 10^{-5}$ mol·mL/g².

molecular weight of these brushes, static light scattering (SLS) measurements were performed in THF. Figure 2 shows a Zimm plot of the brush with PS core and P*t*BA shell (P[S₂₃-*b*-(tBA)₄₆Br]) in THF.

Figure 3 shows the ¹H NMR spectra for the polymers of PBIEM, P(S_{*m*}Br), P[(tBA)_{*n*}Br], P[S_{*m*}-*b*-(tBA)_{*n*}Br], and P[(tBA)_{*n*}-*b*-S_{*m*}Br]. In Figure 3A, no peaks were observed at 3.81 ppm, assigned to methylene protons adjacent to the hydroxy group in poly(HEMA). This indicates the successful esterification of poly(HEMA) with 2-bro-

moisobutyryl bromide. The peaks (a and a') at 4.31 and 4.14 ppm represent the methylene protons adjacent to the ester group in PBIEM. Interestingly, after ATRP of styrene initiated by PBIEM, these two peaks disappear completely while new peaks, b, c, d, and e, representing phenylic protons, end group protons (–CH(Ph)Br), methylene/methine protons in the PS, and methyl groups at the α-end of PS chains appear as shown in Figure 3B, indicating the successful formation of the polymer brush with PS side chains (P(S_{*m*}Br)). Obviously, the terminal benzyl bromide of every side chain of P(S_{*m*}Br) can initiate further ATRP of *t*BA, forming the PS-*b*-P*t*BA side chains. Figure 3C shows the ¹H NMR spectrum of this brush. As can be seen, the peak (c in Figure 3B) at 4.4 ppm disappears completely, and new peaks (peak g at 2.17 ppm and peak f at 4.13–3.96 ppm) appear, which correspond to methine protons in the P*t*BA backbone and end methine protons (–CHBr) at the ω-end of the diblock copolymer side chains, respectively. This demonstrates the successful formation of the brush with diblock copolymer side chains. The formation of the brush with P*t*BA-*b*-PS side chains is also confirmed by the disappearance of the peaks h at 4.13–3.96 ppm for the end groups of poly(macromultiator) in Figure 3D and the appearance of a new peak j for phenylic protons in Figure 3E.

Hydrolysis of the Brush with PS Side Chain.

Detachment of arms from the core has been used for the characterization of star polymers.^{16,18,19} In our case the side chains can be detached from the poly(methacrylate) backbone by basic hydrolysis of the ester group. Subsequent characterization of the free side chains can give information on inter/intra macromolecular coupling reactions. Therefore, the brush with PS side chains was hydrolyzed using KOH in a mixture of THF and ethanol. The SEC traces of the starting brush and the hydrolyzed product are given in Figure 4. The monomodal character and the narrow distribution (PDI = 1.16) of the detached PS side chains substantiate the well-controlled ATRP of styrene initiated by PBIEM as well as the formation of a well-defined polymer brush. Meanwhile, the SEC results also show the absence of

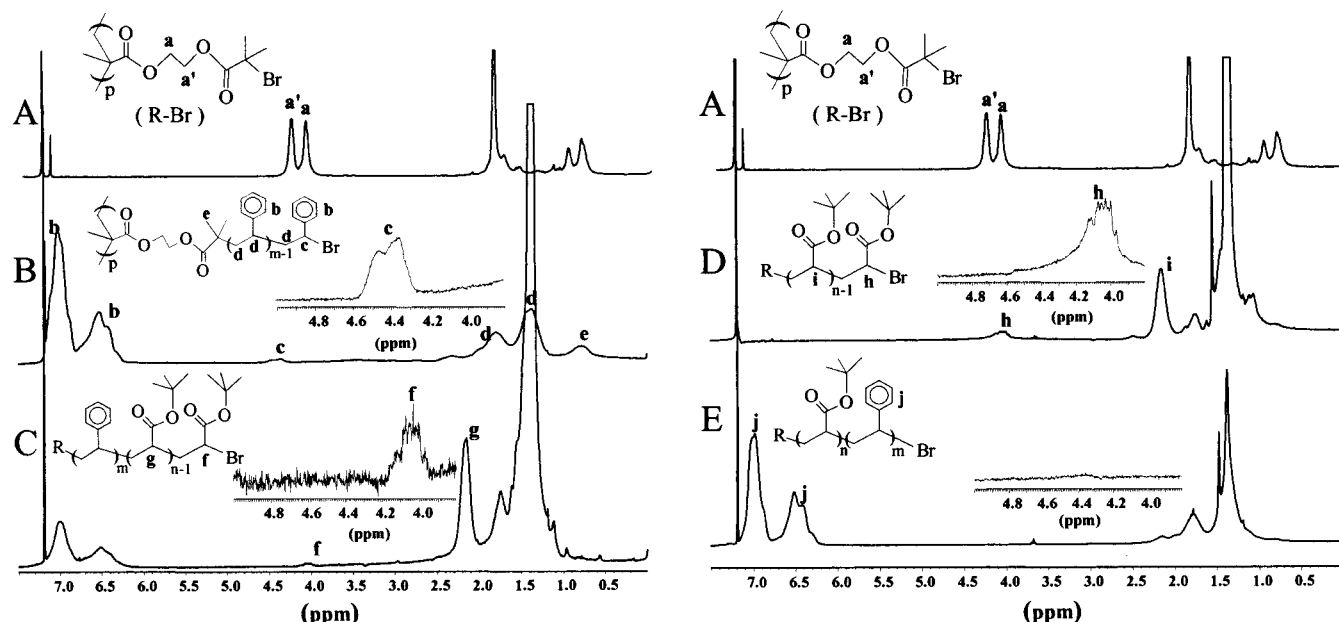


Figure 3. ¹H NMR spectra for PBIEM and the polymer brushes: (A) polyinitiator (PBIEM); (B) P(S₂₃Br); (C) P[S₂₃-*b*-(tBA)₁₈₆Br]; (D) P[(tBA)₁₉Br]; (E) P[(tBA)₁₉-*b*-S₈₁Br].

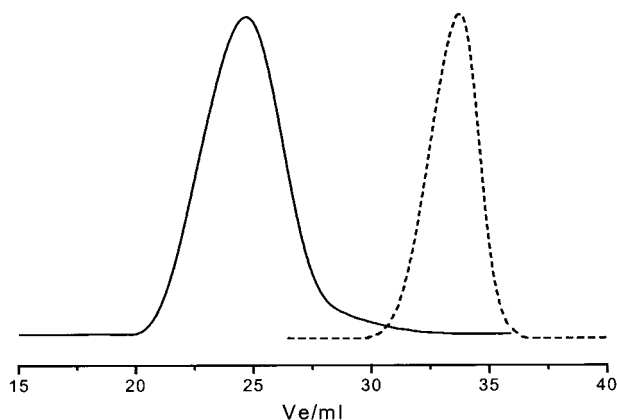


Figure 4. GPC traces of $P(S_{23}Br)$ (—) and the detached PS side chains (---).

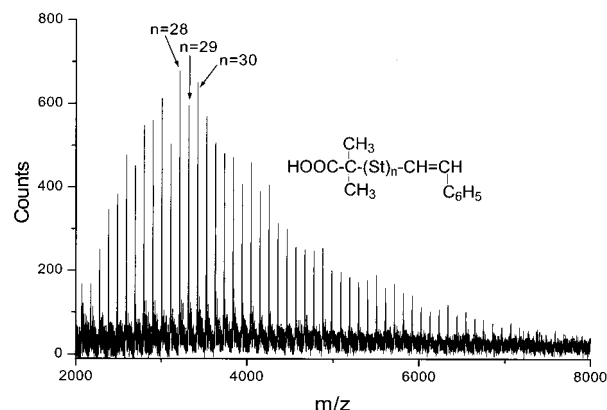


Figure 5. MALDI-TOF mass spectrum of the hydrolyzed PS side chains of the brush $P(S_{23}Br)$.

inter/intramolecular coupling reactions, which was further confirmed by MALDI-TOF analysis of the detached PS side chains as shown in Figure 5. Furthermore, the ratio between the molar masses of the brush ($M_{w,SLS} = 1.20 \times 10^6$) and the detached PS side chain ($M_{w,GPC} = 3850$) was found to be very close to 310, confirming that nearly 100% initiation efficiency of PBIEM was reached during the polymerization. However, it was noted that the M_n of side chains by this method is much higher than that from the NMR spectra of the starting PS brush. For example, the calculated DP_n from the area ratio of peaks b to e (see Figure 3B)

before and after hydrolysis is 12 and 24 respectively, indicating some loss of the signals for phenylic protons in the PS brush. We assume that it indicates a higher density of PS near the polymethacrylate backbone, decreasing the mobility of phenyl protons in the repeating units near to the backbone.

SFM Characterization of Block Copolymer Brushes. The block copolymer brushes were then further characterized by scanning force microscopy (SFM). For this end, dip-coated films were prepared from dilute toluene solutions onto SiO_x or mica surfaces. SFM experiments using silicon oxide surfaces in most cases exhibited dropletlike aggregates instead of single macromolecules, for the brushes with both homopolymer and diblock copolymer side chains. We believe this is mainly due to the lower surface polarity of the silicon surface and the subsequent faster lateral movement of the molecules on the surface during the evaporation process, often leading to dewetting patterns. Thus, for further SFM experiments mica was used as substrate since mica surfaces are charged decreasing the lateral movement of chains.

Figure 6 presents an SFM tapping mode image of $P[S_{23}-b-(tBA)_{186}Br]$ on a mica surface. Single wormlike macromolecules can be visualized directly, and no aggregates are observed. The dimensions of 520 molecules were measured manually without correcting for the tip radius of curvature (≈ 10 nm). The number-average length, the weight-average length, the average diameter, and the average height of the cylinders in Figure 6 are $l_n = 68.4$ nm, $l_w = 88.1$ nm, $d = 20 \pm 2$ nm, and $h = 2.0 \pm 0.1$ nm respectively, with a polydispersity of lengths, $l_w/l_n = 1.29$ which is close to the polydispersity of the backbone, $M_w/M_n = 1.24$. If we subtract 10 nm (average convolution with tip radius taking into account the relatively low height of the imaged objects and therefore reduced convolution) from the length of every molecule in order to account for the convolution of length and tip diameter, the length averages are $l_n = 58.4$ nm, $l_w = 81.4$ nm, and $l_w/l_n = 1.39$ which is somewhat higher than the polydispersity of the brush, $M_w/M_n = 1.34$. The asymmetry of the cross-section, which was also observed in the case of PS¹¹ and PVB brushes,⁴ is due to the collapse of the polymer chains onto, and the interaction with, the surface after the evaporation of the solvent.

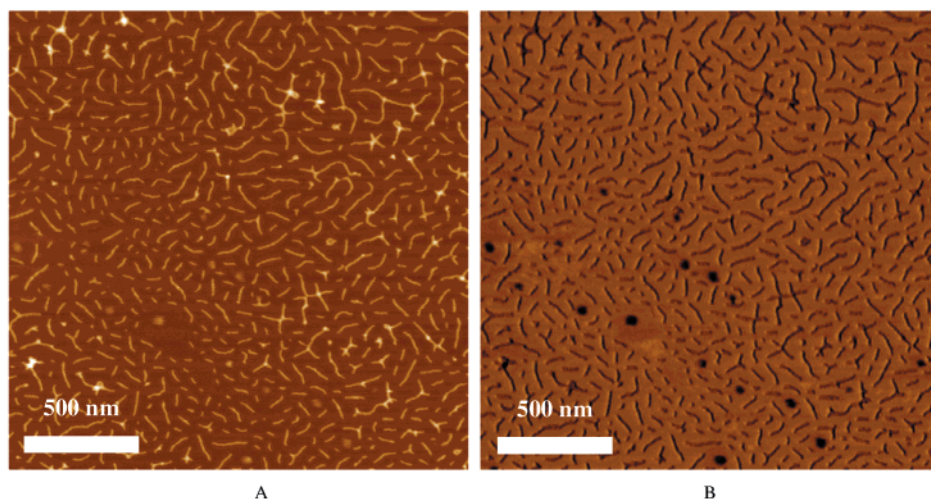


Figure 6. SFM tapping mode image for $P[S_{23}-b-(tBA)_{186}Br]$ dip-coated from toluene onto mica: (A) height (z range: 10 nm) and (B) phase (range = 15°).

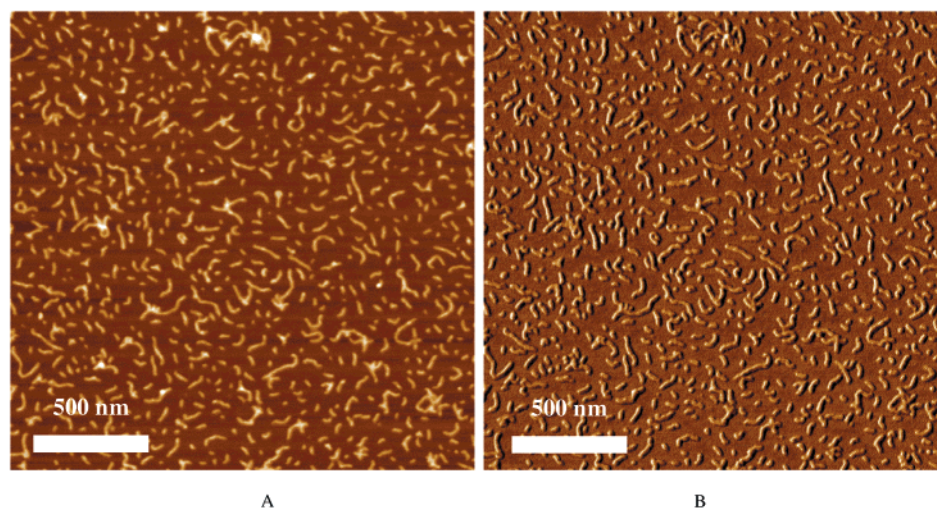


Figure 7. SFM tapping mode image for P[S₂₃-*b*-(AA)₁₈₆Br] dip-coated from chloroform/methanol (volume ratio = 1/1) onto mica: (A) height (*z* range = 10 nm), and (B) phase (range = 15°).

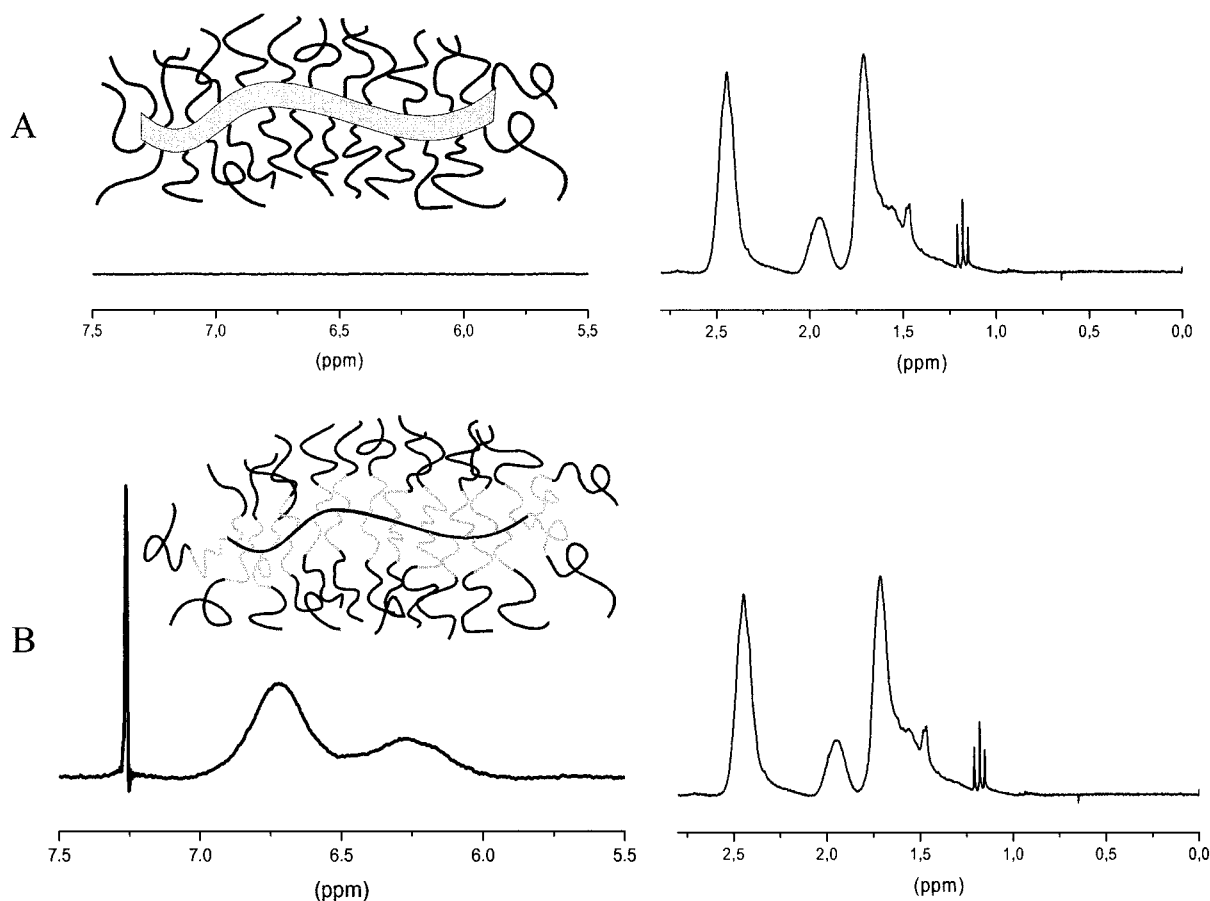


Figure 8. ¹H NMR of P[S₂₃-*b*-(AA)₁₈₆Br]. (A) in CD₃OD, and (B) in CD₃OD/CDCl₃ (volume ratio = 1/1).

Wormlike Unimolecular Micelles with Poly-(acrylic acid) Blocks. The synthesized brushes with PS-*b*-P*t*BA and P*t*BA-*b*-PS side chains were further hydrolyzed in order to obtain wormlike unimolecular micelles of P[S_{*m*}-*b*-(AA)_{*n*}Br] and P[(AA)_{*n*}-*b*-S_{*m*}Br]. From the SFM image of P[S₂₃-*b*-(AA)₁₈₆Br] (Figure 7), we found that the morphology of the single macromolecules was retained after hydrolysis. Figure 8A presents a ¹H NMR spectrum of P[S₂₃-*b*-(AA)₁₈₆Br] obtained in CD₃OD, which is a good solvent for the PAA shell, but a poor solvent for the PS core. The signals of the PAA shell are readily observed indicating an extended conforma-

tion, while no signals of PS are observed, implying the complete collapse of the PS core. By adding about 10 vol % CDCl₃ to this solution, one can restore the PS signals in the spectrum. The PS signals intensify with further addition of CDCl₃. Figure 8B presents the ¹H NMR spectrum for the same polymer in a mixture of CD₃OD/CDCl₃ (volume ratio 1/1). The PS core is solvated by CDCl₃ and therefore remains in an extended conformation. However, the wormlike structure of the micelle is preserved because of the covalent attachment of the PS-*b*-PAA side chains to the backbone. This behavior is very different from that of conventional

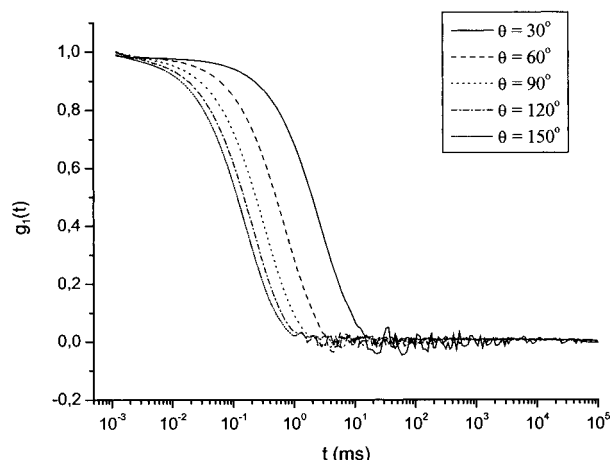


Figure 9. Normalized field correlation functions of P[S₂₃-*b*-(AA)₁₈₆Br] in methanol ($c = 1.0$ g/L) at room temperature at various angles.

dynamic micelles from linear amphiphilic diblock copolymers,²⁰ which are expected to deaggregate or form reverse micelles by changing the solvent quality. It shows that the unimolecular micelles undergo an unisotropic change of dimension by changing the solvent quality.

Dynamic light scattering (DLS) was performed to verify the unimolecular nature of P[S₂₃-*b*-(AA)₁₈₆Br] in both CH₃OH and CH₃OH/CHCl₃ with a concentration of 1.0 g/L at room temperature (Figure 9). The CONTIN analysis²¹ of the autocorrelation functions measured at five different angles for both solvents shows only one peak. After extrapolation to $q^2 \rightarrow 0$, the hydrodynamic radii of the species in CH₃OH and CH₃OH/CHCl₃ was found to be $R_h = 54.6 \pm 1.2$ and 60.4 ± 1.3 nm, respectively. This change is small, but significant, indicating that the increase in width is also reflected in the hydrodynamic radius which for large aspect ratios should be mostly given by the length of the wormlike molecules.

Conclusions

By using ATRP in the "grafting from" process, novel cylindrical brushes with well-defined core-shell structures have been synthesized. The hydrolysis of the core-shell brushes yields interesting amphiphilic polymers which can be regarded as unimolecular wormlike cylindrical micelles. Investigations on these unimolecular amphipolar nanocylinders are in progress and will be published elsewhere.

Acknowledgment. We wish to thank Dr. H. J. Räder (MPI für Polymerforschung, Mainz, Germany) for

the MALDI-TOF MS measurements. A.B. acknowledges a Kekulé fellowship by Stiftung Stipendien-Fonds des Verbandes der Chemischen Industrie and BMBF. This work was partially supported by the Deutsche Forschungsgemeinschaft within the Schwerpunktprogramm "Polyelektrolyte" and SFB 481.

References and Notes

- (1) Tsukahara, Y.; Mizuno, K.; Segawa, A.; Yamashita, Y. *Macromolecules* **1989**, *22*, 1546.
- (2) Tsukahara, Y.; Tsutsumi, K.; Yamashita, Y.; Shimada, S. *Macromolecules* **1990**, *23*, 5201.
- (3) Wintermantel, M.; Gerle, M.; Fischer, K.; Schmidt, M.; Wataoka, I.; Urakawa, K.; Tsukahara, Y. *Macromolecules* **1996**, *29*, 978.
- (4) Dziezok, P.; Sheiko, S. S.; Fischer, K.; Schmidt, M.; Möller, M. *Angew. Chem.* **1997**, *109*, 2894.
- (5) Heroguez, V.; Gnanou, Y.; Fontanille, M. *Macromolecules* **1997**, *30*, 4791.
- (6) Schlüter, A. D. *Top. Curr. Chem.* **1998**, *197*, 165.
- (7) Percec, V.; Ahn, C. H.; Ungar, G.; Yearly, D. S. P.; Möller, M.; Sheiko, S. S. *Nature (London)* **1998**, *391*, 161.
- (8) Gerle, M.; Fischer, K.; Schmidt, M.; Roos, S.; Müller, A. H. E.; Sheiko, S.; Möller, M. *Macromolecules* **1999**, *32*, 2629.
- (9) Ojalali, R.; Hugenberg, N.; Fischer, K.; Schmidt, M. *Macromol. Rapid Commun.* **1999**, *20*, 444.
- (10) Kawaguchi, S.; Akaike, K.; Zhang, Z. M.; Matsumoto, H.; Ito, K. *Polym. J.* **1998**, *30*, 1004.
- (11) Beers, K. L.; Gaynor, S. G.; Matyjaszewski, K.; Sheiko, S. S.; Möller, M. *Macromolecules* **1998**, *31*, 9413.
- (12) (a) Beers, K. L.; Boo, S.; Gaynor, S. G.; Matyjaszewski, K. *Macromolecules* **1999**, *32*, 5772. (b) Robinson, K. L.; Khan, M. A.; de Paz Báñez, M. V.; Wang, X. S.; Armes, S. P. *Macromolecules* **2001**, *34*, 3155.
- (13) Hirao, A.; Kato, H.; Yamaguchi, K.; Nakahama, S. *Macromolecules* **1986**, *19*, 1294.
- (14) Wang, J. S.; Matyjaszewski, K. *J. Am. Chem. Soc.* **1995**, *117*, 5614.
- (15) Cheng, G.; Simon, P. F. W.; Hartenstein, M.; Müller, A. H. E. *Macromol. Rapid Commun.* **2000**, *21*, 846.
- (16) Angot, S.; Murthy, K. S.; Taton, D.; Gnanou, Y. *Macromolecules* **1998**, *31*, 7218.
- (17) Spickermann, J.; Räder, H. J.; Müllen, K.; Müller, B.; Gerle, M.; Fischer, K.; Schmidt, M. *Macromol. Rapid Commun.* **1996**, *17*, 885.
- (18) Jacob, S.; Majoros, I.; Kennedy, J. P. *Macromolecules* **1996**, *29*, 8631.
- (19) Hawker, C. J. *Angew. Chem.* **1995**, *107*, 1623.
- (20) Zhang, L.; Shen, H.; Eisenberg, A. *Macromolecules* **1997**, *30*, 1001.
- (21) Provencher, S. W. *Comput. Phys. Commun.* **1982**, *27*, 229.
- (22) During the revision of this paper, H. G. Börner et al.²³ published the synthesis of molecular brushes with PS-*b*-poly(*n*-butyl acrylate) and poly(*n*-butyl acrylate)-*b*-PS side chains using a similar strategy.
- (23) Börner, H. G.; Beers, K.; Matyjaszewski, K.; Sheiko, S. S.; Möller, M. *Macromolecules* **2001**, *34*, 4375.

MA0013962